Kian Eisazadeh-Far

Hameed Metghalchi
e-mail: metghalchi@coe.neu.edu

Mechanical and Industrial Engineering Department,
Northeastern University,
Boston, MA 02115

James C. Keck
Mechanical Engineering Department,
Massachusetts Institute of Technology,
Cambridge, MA 02139

Thermodynamic Properties of Ionized Gases at High Temperatures

Thermodynamic properties of ionized gases at high temperatures have been calculated by a new model based on local equilibrium conditions. Calculations have been done for nitrogen, oxygen, air, argon, and helium. The temperature range is 300–100,000 K. Thermodynamic properties include specific heat capacity, density, mole fraction of particles, and enthalpy. The model has been developed using statistical thermodynamics methods. Results have been compared with other researchers and the agreement is good.
[DOI: 10.1115/1.4003881]

Keywords: thermodynamic properties, ionized gases, high temperature, plasma

1 Introduction

The purpose of this paper is to provide the thermodynamic properties of nitrogen, oxygen, air, argon, and helium at high temperatures. These properties are needed for the study of spark discharges where the electrical energy is deposited in a small kernel and converted to thermal energy in the gas. This is a high temperature process leading to the formation of plasmas with very high degrees of ionization. The initial processes and the mechanisms of plasma kernel formation are beyond the scope of this paper and more details can be found in other references [1–5]. However, as the electrical energy is converted to the thermal energy, the temperature of the plasma increases rapidly and the kernel grows. It is to calculate this growth process that the thermodynamic properties of the plasma, in particular, the specific heat capacity at constant pressure, are needed.

Prior calculations of the thermodynamic properties of high temperature plasmas have been carried out by several investigators using a variety of models. Capitelli et al. [6] have calculated the thermodynamic properties of air at high temperature using empirical correlations. They calculated the specific heat capacity, density, molecular weight, thermal conductivity, viscosity, entropy, enthalpy, and mole fraction of species over the temperature range 50,000 to 100,000 K. Giordano et al. [7] have calculated the thermodynamic properties using statistical mechanical methods. Yos [8] calculated the transport properties of air and its constituents in the temperature range 300–30,000 K. Sher et al. [9] studied the birth of spark channels. For this purpose, they calculated the specific heat capacity and mole fractions of the air at high temperatures using a simplified thermodynamic model but their results are not very accurate. Other studies performed in last few decades include Behringer et al. [10], Jordan and Swift [11], Kopainsky [12], and Pateyron et al. [13]. Most of these calculations cover the properties up to 50,000 K. However, for plasmas other than air, such as the inert gases helium and argon, the available data in temperature range up to 100,000 K is limited.

In this paper, we present a new model based on statistical mechanics which is both simple and accurate. Calculations have been made for nitrogen, oxygen, air, argon, and helium. The temperature range is 300–100,000 K at constant atmospheric pressure. The calculated properties include specific heat capacity, density, enthalpy, and the number of particles. Results have been compared with existing prior data and where the conditions overlap the agreement is generally good.

2 General Model

The general model is based on statistical thermodynamic methods and it is assumed that the species are in thermodynamic equilibrium. The physical constants of the ions and species are taken from Fay [14] and Moore [15]. For nitrogen, oxygen, and air, the considered species are N_2, N, N^+, N^{2+}, N^{3+}, N^{4+}, N^{5+}, N^{6+}, O_2, O, O^+, O^{2+}, O^{3+}, O^{4+}, O^{5+}, O^{6+}, O^{7+}, and e (electron). In addition to nitrogen, oxygen, and air plasma, the properties of two inert gases, argon and helium, have been studied as well. The assumed species for argon are Ar, Ar^+, Ar^{2+}, Ar^{3+}, Ar^{4+}, Ar^{5+}, and Ar^{6+} and for helium are He, He^+, and He^{2+}.

We assume a diatomic gas at low temperatures. The number of elemental atom number is then given by

$$EA = 2A_2 + \sum_{\varepsilon=0}^{z} A^{\varepsilon} \quad \varepsilon = 0, 1, 2, 3, ..., z \tag{1}$$

where ε is the charge number of the ions.

Total number of moles is given by

$$M_A = A_2 + e + \sum_{\varepsilon=0}^{z} A^{\varepsilon} \tag{2}$$

Assuming charge neutrality, the mole number of free electrons is given by

$$e = \sum_{\varepsilon=0}^{z} \varepsilon A^{\varepsilon} \tag{3}$$

The equation of state is

$$pV = M_A RT \tag{4}$$

where p is the pressure, V is the volume, R is the universal gas constant, and T is the temperature.

2.1 Dissociation. For a dissociation reaction,

$$A_2 \rightarrow 2A + \Delta H_d, \tag{5}$$

ΔH_d is the dissociation enthalpy. The equilibrium constant based on concentration is defined by

Contributed by the Advanced Energy Systems Division of ASME for publication in the JOURNAL OF ENERGY RESOURCES TECHNOLOGY. Manuscript received April 26, 2010; final manuscript received February 25, 2011; published online May 26, 2011. Assoc. Editor: Muhammad M. Rahman.

$$K_{ed} = \frac{A^2}{A_2 V} \tag{6}$$

Using Eq. (4) to eliminate V in Eq. (6) we obtain

$$\frac{A^2}{A_2 M} = \frac{K_{ed} RT}{p} = \frac{K_{pd}}{p} \tag{7}$$

At low temperature there are no ions ($e \approx 0$), and Eqs. (1) and (2) reduce to

$$A_2 = (EA - A)/2 \tag{8}$$

$$M_A = (EA + A)/2 \tag{9}$$

Substituting Eqs. (8) and (9) in Eq. (7) we will have

$$4B_d y^2 = 1 - y^2 \tag{10}$$

where

$$y = A/EA \tag{10a}$$

$$B_d = p/K_{pd} \tag{10b}$$

and K_{pd} is the equilibrium constant based on pressure.

Solving Eq. (10) we obtain

$$y_0 = (1 + 4B_d)^{-1/2} \tag{11}$$

where

$$y_0 = \sum_{\varepsilon=0}^{z} y^{\varepsilon} \tag{12}$$

From Eqs. (8) and (9)

$$y_2 = \frac{A_2}{EA} = \frac{1 - y_0}{2} \tag{13}$$

Figure 1 shows the variation of y_0, y_2, and M_A/EA for nitrogen dissociation. The normalized number of moles M_A/EA, increases due to dissociation of the molecule to atoms. The concentration of y must decrease at higher temperatures due to ionization. In the Sec. Ionization process, ionization process will be described to complete the predictions.

2.2 Ionization Process. The governing equations for ionization will now be described.

For a typical ionization reaction

$$A^{\varepsilon-1} \rightarrow A^{\varepsilon} + e + \Delta H_{\varepsilon} \quad \varepsilon = 0, 1, 2, 3, ..., z \tag{14}$$

ΔH_{ε} is the ionization enthalpy. The equilibrium constant based on concentration is given by

$$K_{ei} = \frac{A^{\varepsilon} e}{A^{\varepsilon-1} V} \tag{15}$$

Using Eq. (4) to eliminate V in Eq. (15) we obtain

$$\frac{A^{\varepsilon} e}{A^{\varepsilon-1} M} = \frac{K_{ei} RT}{p} = \frac{K_{pi}}{p} \tag{16}$$

The number of elemental atoms involved in reaction (14) is

$$EA = A^{\varepsilon-1} + A^{\varepsilon} \tag{17}$$

The total mole numbers is

$$M_A = EA + e \tag{18}$$

The number of moles of electrons is

$$e = (\varepsilon - 1)A^{\varepsilon-1} + \varepsilon A^{\varepsilon} \tag{19}$$

Combining Eqs. (17)–(19), we obtain

$$A^{\varepsilon-1} = EA - A^{\varepsilon} \tag{20}$$

$$M_A = \varepsilon EA + A^{\varepsilon} \tag{21}$$

$$e = (\varepsilon - 1)EA + A^{\varepsilon} \tag{22}$$

Substituting Eqs. (20)–(22) in Eq. (16) then gives

$$(y^{\varepsilon})^2 + (\varepsilon - 1)y^{\varepsilon} - \frac{\varepsilon}{1 + B_{\varepsilon}} = 0 \tag{23}$$

Solving this second-order equation, we find

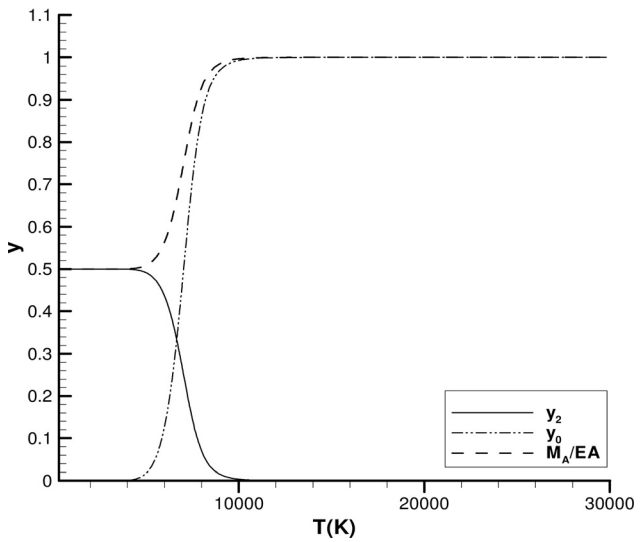

Fig. 1 The variation of y_0, y_2, and M_A/EA versus temperature during the dissociation process

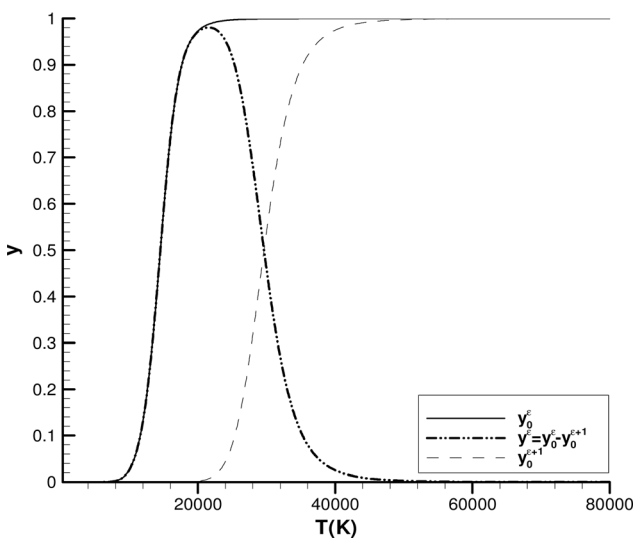

Fig. 2 Variation of y_0^{ε}, $y_0^{\varepsilon+1}$, y^{ε} versus temperature during the ionization process

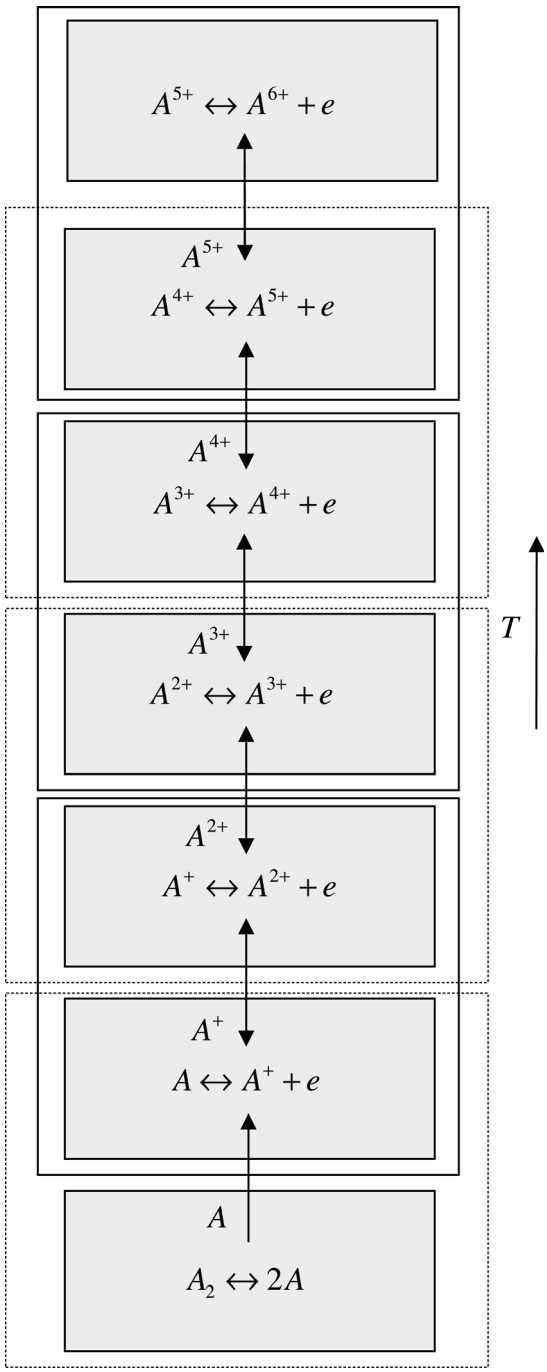

Fig. 3 The sketch of equilibrium packages

$$y_0^{\varepsilon} = \frac{1}{2}\left\{\left[(\varepsilon-1)^2 + \frac{4\varepsilon}{1+B_{\varepsilon}}\right]^{1/2} - (\varepsilon-1)\right\} \tag{24}$$

$$y_0^{\varepsilon} = y^{\varepsilon} + y^{\varepsilon+1} + \cdots + y^{z} \tag{25}$$

$$y^{\varepsilon} = y_0^{\varepsilon} - y_0^{\varepsilon+1} \tag{26}$$

It can be seen in Eq. (25) that y_0^{ε} involves the potential concentration of other ions in upper levels; so it increases and eventually reaches unity. The actual concentration of y^{ε} is achieved by correcting y_0^{ε} in Eq. (26) by taking into account the effect of next ionization. Figure 2 shows the variations of y^{ε}, y_0^{ε} and $y_0^{\varepsilon+1}$ versus temperature during the ionization process. The physical basis of this model is that ionization is an endothermic process and the

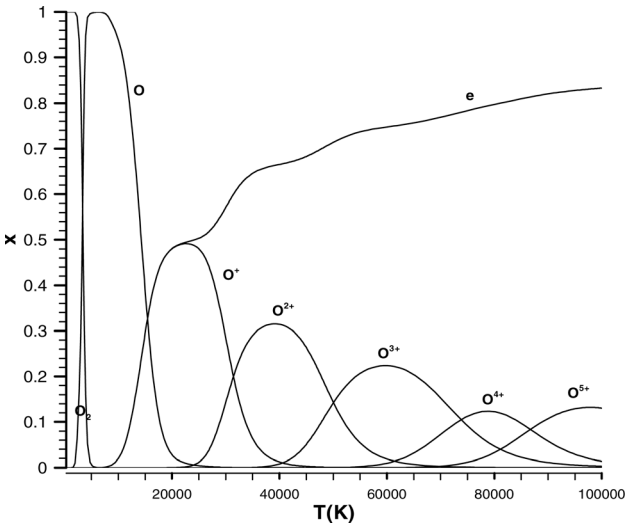

Fig. 4 Mole fractions of oxygen species versus temperature ("e" represents the electron)

progress of each reaction requires additional energy. Therefore, it can be assumed that ionization is a step by step process and the level of ionization increases with temperature.

Figure 3 shows the sketch of this model. The calculations are performed in parallel and the individual packages are in mutual equilibrium. The starting point is the bottom package ($A_2 \leftrightarrow 2A$). The normalized mole fraction of A versus elemental number of nitrogen atoms is entered to the next package and the calculations proceed; in the next package, the output will be A^+ and the same pattern flows to the next ones. In each package, thermodynamic equilibrium calculations are performed and the concentration of each species is computed. The mole fractions of species are normalized by the elemental number of atoms to ensure the conservation of mass. Given the temperature, pressure, and composition all the thermodynamic properties of the plasma can be calculated.

The enthalpy is defined as

$$H_{\mathrm{A}} = h_{\mathrm{A}_2}(T)A_2 + \sum_{\varepsilon=0}^{z} h^{\varepsilon}(T)A^{\varepsilon} \tag{27}$$

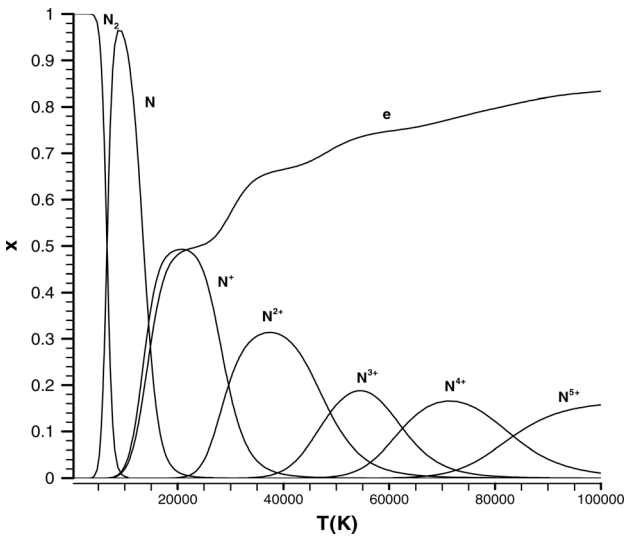

Fig. 5 Mole fractions of nitrogen species versus temperature ("e" represents the electron)

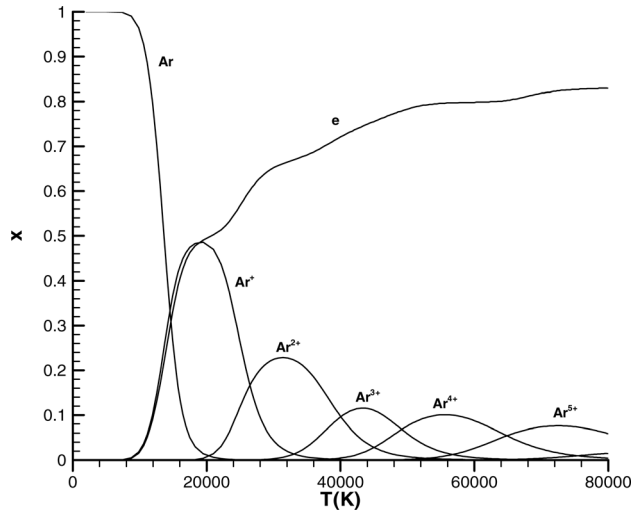

Fig. 6 Mole fractions of argon plasma versus temperature ("e" represents the electron)

where $h_{A_2}(T)$ is the enthalpy of molecule A_2, and $h^{\varepsilon}(T)$ is the enthalpy for species A^{ε}.

Normalized enthalpy will be

$$\frac{H_A}{EA} = h_{A_2}(T)y_2 + \sum_{\varepsilon=0}^{z} h_A^{\varepsilon}(T)y^{\varepsilon} \tag{28}$$

Heat capacity of the mixture is defined by

$$\frac{c_{pA}}{EA} = \left(\frac{\partial H_A/EA}{\partial T}\right)_p = \frac{\partial h_A}{\partial T}y_2 + h_A\frac{\partial y_2}{\partial T} + \sum_{\varepsilon=0}^{z}\left(\frac{\partial h_A^{\varepsilon}}{\partial T}y^{\varepsilon} + h_A^{\varepsilon}\frac{\partial y^{\varepsilon}}{\partial T}\right) \tag{29}$$

c_p is the combination of translational, rotational, vibrational, and electronics energy modes. It is defined by

$$c_p = (c_p)_{\text{translational}} + (c_p)_{\text{rotational}} + (c_p)_{\text{vibrational}} + (c_p)_{\text{electronics}} \tag{30}$$

An important feature of this model is that the properties of the individual ion packages are first calculated and then coupled to form the system of packages. This flexibility permits a wide range of conditions to be covered by just one generic set of equations. For example, the model can treat the system of oxygen plasma, nitrogen plasma, and air plasma simultaneously.

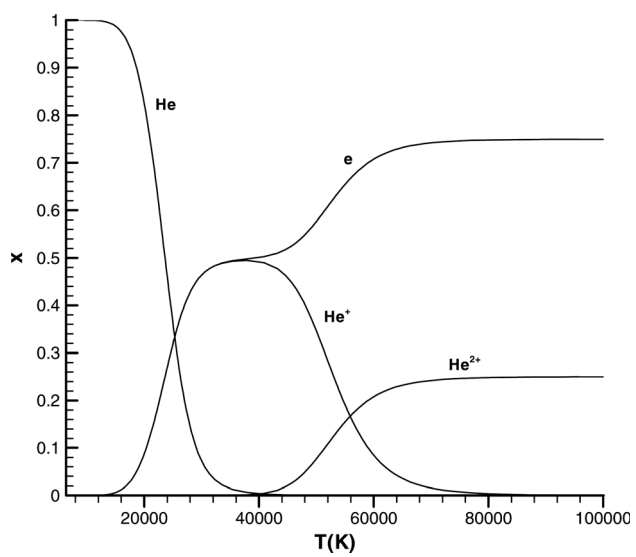

Fig. 7 Mole fractions of helium plasma versus temperature ("e" represents the electron)

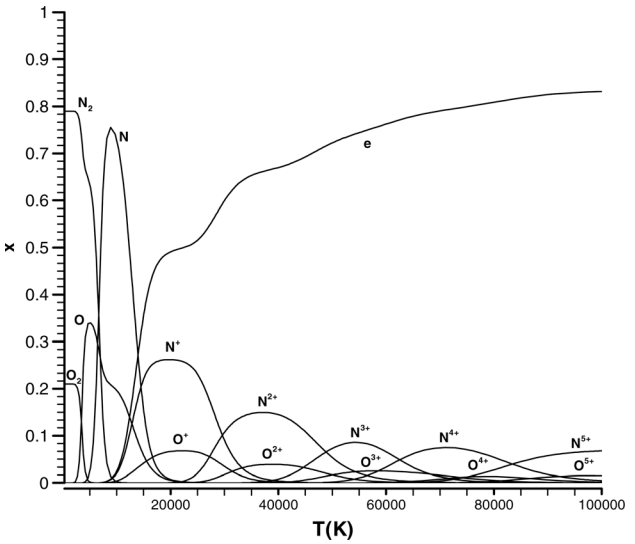

Fig. 8 Mole fractions of air species versus temperature

3 Results and Discussion

Figures 4 and 5 show the mole fractions of oxygen and nitrogen plasma up to 100,000 K. The mole fractions in these two figures are defined by

$$\begin{aligned} x_{A^{\varepsilon}} &= \left(\frac{A^{\varepsilon}}{EA}\right)\Big/\left(\frac{M_A}{EA}\right) \quad \text{for monatomic species and} \\ x_{A_2} &= \left(\frac{A_2}{EA}\right)\Big/\left(\frac{M_A}{EA}\right) \quad \text{for molecule} \end{aligned} \tag{31}$$

It can be seen that for both atoms, one dissociation and five ionizations (N^{5+} and O^{5+}) occur. The onset of ionization occurs around 6000 K, and as the ionization proceeds, the mole fraction of species decrease. This is due to the increasing mole fraction of

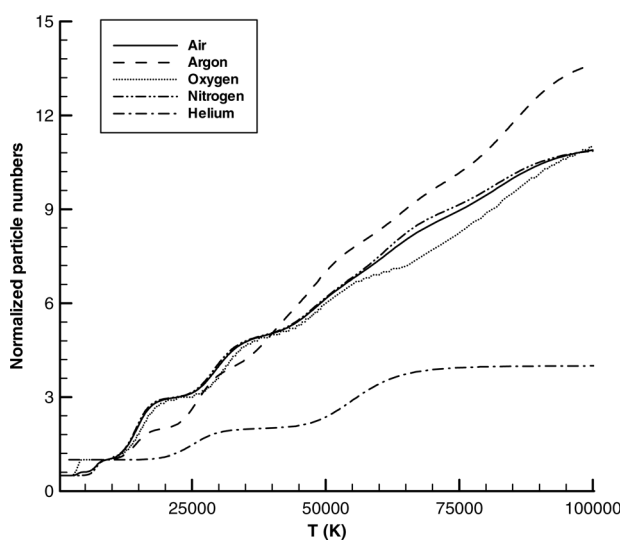

Fig. 9 Plasma particle numbers normalized by elemental atom numbers

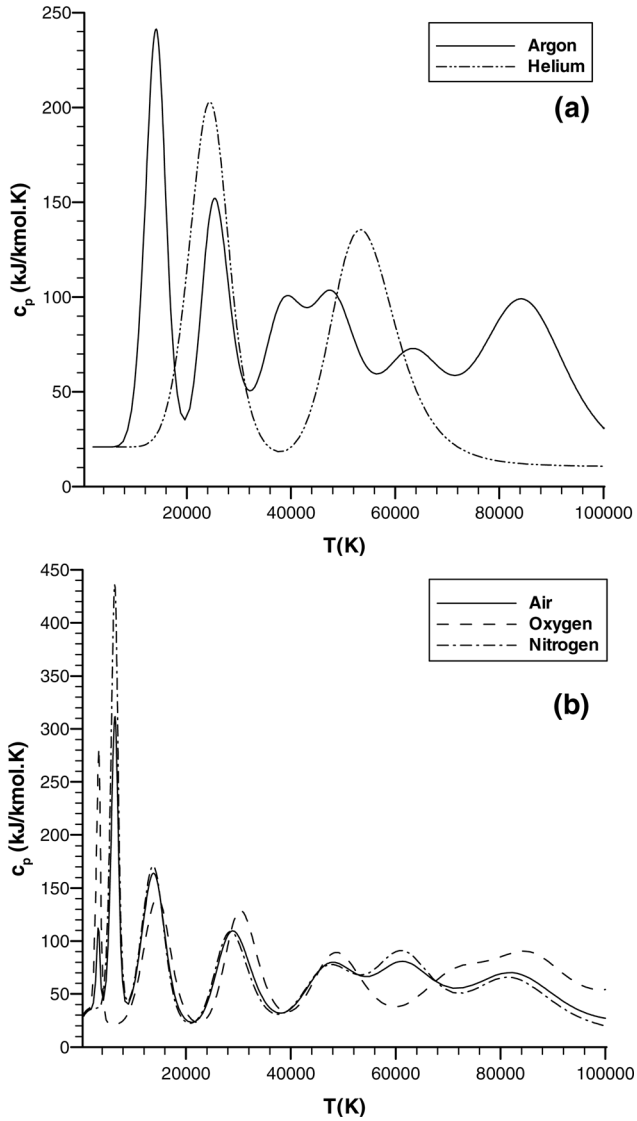

Fig. 10 Heat capacities of oxygen, nitrogen, argon, and helium versus temperature; (*a*) helium and argon, (*b*) air, oxygen, and nitrogen

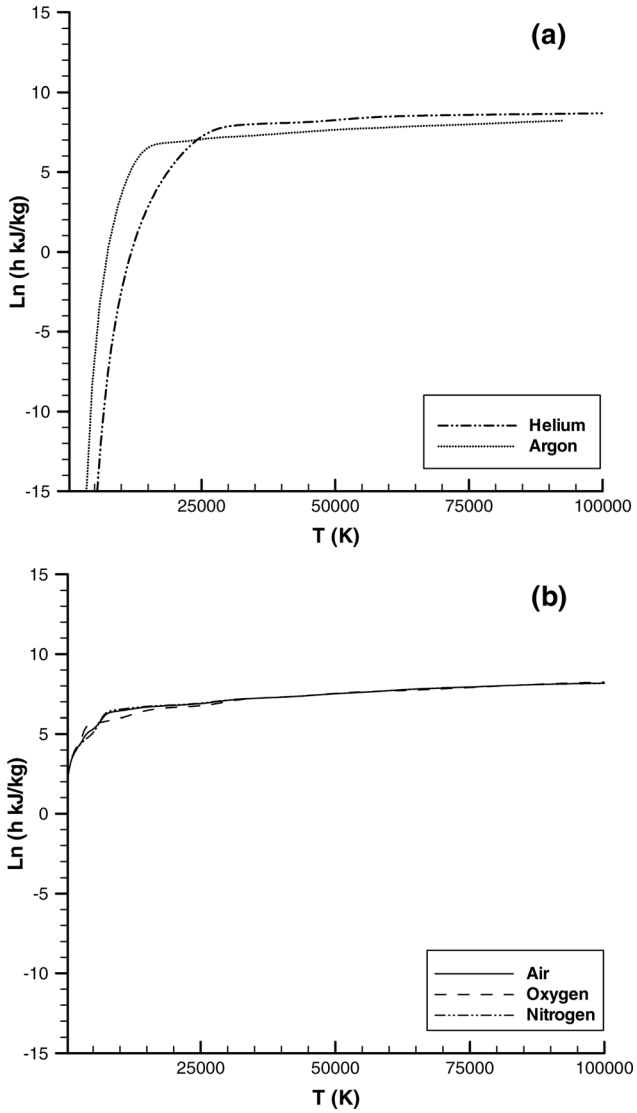

Fig. 11 enthalpies of different species versus temperature; (*a*) argon and helium, (*b*) air, oxygen, and nitrogen

electrons. Figures 6 and 7 show the mole fractions of argon and helium.

Figure 8 shows the mole fractions of air plasma. The peaks of this figure correspond to those in Figs. 4 and 5.

Figure 9 shows normalized particle numbers of oxygen, nitrogen, air, argon, and helium versus temperature. The particle numbers have been normalized by the elemental number of atoms. It can be seen that under constant pressure condition, the number of particles increase dramatically. It shows the effect of ionization and increasing number of electrons. It is seen that the level of ionization determines the number of particles. Since in helium there are just two electrons, the number of particles does not increase as much as for other species.

Figure 10 shows specific heat capacities of oxygen, nitrogen, air, argon, and helium versus temperature. The several peaks at this figure represent the reactions and production of atoms and ions, which increase the heat capacity of the system. For oxygen and nitrogen molecules, the role of rotational and vibrational energy modes on heat capacity is important at lower temperatures. However, after dissociation, the only energy mode of each species is translational and electronic and the increase in the heat capacity is just due to the ionization and the change of species concentration as can be seen in Eq. (29).

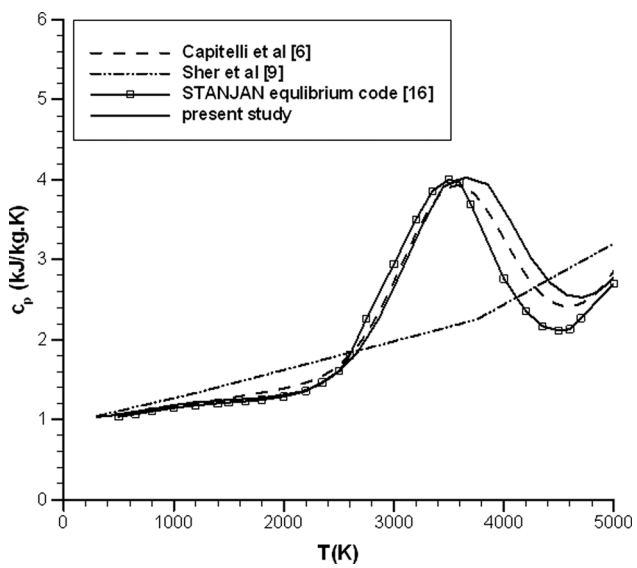

Fig. 12 Heat capacity of air versus temperature and comparison with other researchers (300–5000 K); - - - -, Ref. 6; – · · –, Ref. 9; —□—, Ref. 16; ——, present study

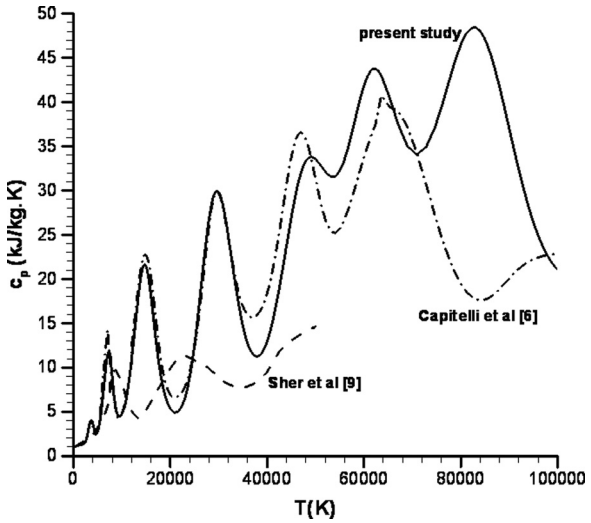

Fig. 13 Heat capacity of air versus temperature and comparison with other researchers (300–100,000 K); -·-·-, Ref. 6; - - - -, Ref. 9; ——, present study

A comparison between Figs. 4–8 and Fig. 10 shows that the peak values of heat capacities correspond to the stage where the rate of dissociation and ionization is maximum. For example for air, first two peaks represent the equilibrium reaction of oxygen and nitrogen molecules and atoms and the rest of peaks correspond to the ionization reactions. Since there are just two ionization reactions in helium, consequently, only two peaks are observed in the figure. The behavior of this figure can be understood by the terms appeared in Eq. (29).

Figure 11 shows enthalpies of oxygen, nitrogen, air, argon, and helium versus temperature. At higher temperatures, the enthalpy of helium exceeds the enthalpy of air. This is due to the higher heat capacity of helium at higher temperatures.

4 Comparison With Other Calculations

Figure 12 shows values of specific heat and the comparison with the results of Capitelli et al. [6], Sher et al. [9], and STANJAN equilibrium code [16] in temperature range of 300–5000 K. Except for Sher et al., the agreement is good. In this range of temperature, the concentration of ions is almost zero and the increase in heat capacity is due to the excitement of the vibrational energy modes and dissociation of oxygen atom.

Figure 13 compares the heat capacities of air calculated in this study with those of Capitelli and Sher over the temperature range 300–100,000 K. This figure shows good agreement with the results of Capitelli up to 70,000 K. Beyond 70,000 K, Capitelli et al. underestimates the heat capacity due to the neglect of the N^{5+} and O^{5+} ions in their study. Results of Sher are limited to low temperatures that are in poor agreement with the others.

5 Conclusions

Thermodynamic properties of air, argon, and helium have been calculated at high temperatures using a novel cascade thermodynamic model. It was assumed that all species are in local thermodynamic equilibrium. The model is based on statistical thermodynamics methods.

The calculated properties are specific heat capacity, enthalpy of the mixture, mole fraction of species, particle numbers, and density. It is shown that all these properties are very temperature sensitive. It is also shown that number of ions and ionization level play an important role in determining specific heat capacities and particle numbers in the mixture. Results are compared with those of other researchers and good agreement is obtained in regions where the results overlap.

Acknowledgment

This research has been supported by the Office of Naval Research (ONR) grant number N00010-09-1-0479. The authors are thankful for the technical monitoring of Dr. Gabriel Roy.

Nomenclature

A = the number of atom A
c_p = specific heat capacity
e = mole number of electron
EA = number of elemental atom A
h = specific enthalpy
H = total enthalpy
K = equilibrium constant
M = total number of moles
P = pressure
R = gas constant
T = temperature
V = volume
x = mole fraction
z = total charge of the element
x = mole fraction

Greek Letters

ε = charge

Superscripts

z = total charge of the element
ε = charge of the species

Subscripts

A = atom A
d = dissociation
e = equilibrium
d = dissociation
p = constant pressure

References

[1] Bradley, D., Sheppard, C. G. W., Suardjaja, I. M., and Woolley, R., 2004, "Fundamentals of High-Energy Spark Ignition with Lasers," Combust. Flame, **138**(1–2), pp. 55–77.
[2] El-Koramy, R. A., Effendiev, A. Z., and Aliverdiev, A. A., 2007, "The Peculiarities of Spark Channel Formation in Air Gas at Atmospheric Pressure," Physica B, **392**(1–2), pp. 304–308.
[3] Kravchik, T., and Sher, E., 1994, "Numerical Modeling of Spark Ignition and Flame Initiation in a Quiescent Methane-Air Mixture," Combust. Flame, **99**(3–4), pp. 635–643.
[4] Maly, R., 1981, "Ignition Model for Spark Discharges and the Early Phase of Flame Front Growth," Sym. (Int.) Combust., **18**(1), pp. 1747–1754.
[5] Schäfer, M., Schmidt, R., and Köhler, J., 1996, "I-D Simulation of a Spark Discharge in Air," Sym. (Int.) Combust., **26**(2), pp. 2701–2708.
[6] Capitelli, M., Colonna, G., Gorse, C., and D'Angola, A., 2000, "Transport Properties of High Temperature Air in Local Thermodynamic Equilibrium," Eur. Phys. J. D, **11**, pp. 279–289.
[7] Giordano, D., Capitelli, and M., Colonna, G., 1994, *Tables of Internal Partition Functions and Thermodynamic Properties of High-Temperature Air Species From 50 K to 100000 K*, European Space Agency (ESA), Paris, 237.
[8] Yos, J. M., 1963, "Transport Properties of Nitrogen, Hydrogen, Oxygen, and Air to 30,000 Degrees K," Avco Corp., Tech. Memo. RAD-TM-63-7, pp. 71.
[9] Sher, E., Ben-Ya'Ish, J., and Kravchik, T., 1992, "On the Birth of Spark Channels," Combust. Flame, **89**(2), pp. 214–220.
[10] Behringer, K., Kollmar, W., and Mentel, J., 1968, "Messung der Wärmeleitfähigkeit von Wasserstoff Zwischen 2000 und 7000 °K," Z. Phys. **215**, pp. 127–151.
[11] Jordan, D., and Swift, J. D., 1973, "Measurement of Thermal Conductivity of Argon-Nitrogen Gas Mixtures at High Temperatures," Int. J. Electron.," **35**(5), pp. 595–608.
[12] Kopainsky, J., 1971, "Strahlungstransportmechanismus und Transportkoeffizienten im Ar-Hochdruckbogen," Z. Phys, **248**(5), pp. 417–432.
[13] Pateyron, B., Elchinger, M. F., Delluc, G., and Fauchais, P., 1992, "Thermodynamic and Transport Properties of Ar–H2 and Ar–He Plasma Gases Used for Spraying at Atmospheric Pressure," Plasma Chem. Plasma Process., **12**(4), pp. 421–448.
[14] Fay, J., 1965, *Molecular Thermodynamics*, Allison-Wesley, Reading, MA.
[15] Moore, C. E., 1971, "Atomic Energy Levels," U.S. Department of Commerce, National Bureau of Standards, NSRDS-NBS 35, Vol. 1.
[16] Reynolds, W. C., 1980, STANJAN Interactive Computer Programs for Chemical Equilibrium Analysis, Stanford University